



OPEN Exploring agglomeration of respirable silica and other particles in coal mine dust

Emily Sarver[✉], Daniel Sweeney, Lizeth Jaramillo Taborda & Cigdem Keles

A better understanding of respirable dust particle characteristics is needed to advance exposure monitoring and prevent health effects. In coal mines and other occupational environments, understanding respirable silica is especially important. Scanning electron microscopy with energy-dispersive X-ray spectroscopy (SEM-EDX) enables particle-level dust analysis, but interpretation of data can be challenging when samples include agglomerated particles (i.e., particulates consisting of multiple independent particles attached together). On the other hand, a failure to recognize agglomerates or account for them in analysis risks oversimplification in exposure assessment. This research explores possible effects of agglomerates on respirable coal mine dust classification by SEM-EDX, with a specific focus on silica. Analysis was conducted both on respirable samples (collected with a typical apparatus including a cyclone size selector) and on respirable-sized particulates identified in passive samples. Results demonstrate that silica is often contained in respirable-sized agglomerates, though the typical respirable sampling apparatus appears to break up some of those agglomerates. For agglomerates that do persist, they may influence SEM-EDX results—possibly increasing apparent size distributions and/or “hiding” some of their constituents, including silica.

Respirable crystalline silica is well-established as an occupational health hazard^{1–7}. In coal mine environments, it normally occurs as quartz and represents just one constituent of the respirable dust fraction, which can include other minerals (e.g., silicates, carbonates, metal oxides and sulfides), coal dust and diesel particulates^{8,9}. Chronic exposure to respirable coal mine dust (RCMD) can lead to a spectrum of lung diseases, most notably Coal Workers’ Pneumoconiosis (CWP, or “Black Lung”) ¹⁰. Crystalline silica, in particular, is considered a key agent in the most severe form of CWP, which is called progressive massive fibrosis (PMF)¹¹.

Given the known hazard, respirable silica exposure is widely regulated in occupational environments¹². In coal mines, regulatory compliance is determined based on routine monitoring which tracks mass concentration of quartz using RCMD filter sample analysis¹². In the United States, the available monitoring data indicate that quartz concentrations have declined since Federal regulations were implemented in the early 1970s^{13,14}. However, health surveillance and Federal benefits data show a dramatic resurgence of PMF, especially in the central Appalachian region, which began in the late 1990s and is still ongoing^{15,16}. This contradiction suggests compliance monitoring might not yield sufficient understanding of the risks posed by exposure—and indeed this is not the explicit goal of compliance monitoring.

Related to silica dust analysis, more insight may be needed on the relevant characteristics of particles that could impart relatively high toxicity despite relatively low mass concentration¹². For example, reduced particle size has implications for particle mobility, deposition, and toxicity in the lung^{17,18}. Using scanning electron microscopy with energy dispersive X-ray spectroscopy (SEM-EDX) to analyze RCMD samples from 25 underground US mines, the authors have found that silica particles are predominantly submicron—and are generally finer than other mineral particles¹⁹. Further, silica particles are typically most abundant and finest near active drilling/cutting activities, especially in thin-seam mines¹⁹. (It is noted that SEM-EDX can be used to evaluate particle chemistry to infer silica composition, however the technique cannot be used to determine crystalline structure in order to report quartz (or other forms of silica), per se.)

The nature of silica particle surfaces could also be an important determinant in toxicity²⁰. Of the surface characteristics that might be expected to vary within a mine environment, the degree of particle liberation/occlusion is thought to influence the lung response^{21–24}. As a simple conceptualization: whereas a liberated or “free” silica particle is expected to have relatively clean and reactive surfaces (i.e., as commonly conceptualized in silicosis pathology⁵, an “occluded” particle that is covered by a thin, adherent layer of a less reactive mineral (e.g., aluminosilicate clay) might ameliorate toxicity to some extent²². To distinguish occluded versus free silica particles in well-dispersed samples, Wallace et al. (1990) demonstrated a method using SEM-EDX to sense

Department of Mining and Minerals Engineering, Virginia Tech, Blacksburg, VA, USA. ✉email: esarver@vt.edu

changes in a particle's elemental composition from its surface to core²⁵; and Harrison et al. (1996) used the method to show that both occluded and free silica particles occurred in RCMD from various geographic regions of the US²⁶. As part of an investigation of respirable silica in 15 contemporary US coal mines, the authors previously attempted to apply the same SEM-EDX method directly on RCMD filter samples (i.e., as collected, with no sample preparation to promote particle dispersion)²⁷. While both occluded and free silica particles were identified, the direct-on-filter analysis was frequently confounded by the presence of agglomerates which contained respirable silica along with other particles—typically aluminosilicates or coal dust. Notably, these agglomerates were still in the respirable size range, with most being less than about 5 μm .

Agglomerates in RCMD

Agglomerates, in general, have been documented in the context of RCMD. In a 1988 study aimed at evaluating sampling techniques, Armbruster²⁸ collected simultaneous samples of total airborne dust and respirable dust in several coal mines. Based on shifts in particle size distributions between the ambient dust (as collected) and the same dust following dispersion (via ultrasonic micro-sieving), Armbruster²⁸ reported the presence of significant agglomerates; and, upon comparing the dispersed and respirable dust samples, concluded that standard respirable sampling (i.e., with a cyclone pre-selector) likely broke up some of the agglomerates. Armbruster discussed this finding with respect to its impact on the representativeness of such samples for evaluating real exposures, since the agglomerates should behave differently than their constituent particles upon inhalation (e.g., in terms of deposition, reactivity). More recent studies have also documented respirable-sized agglomerates in coal mine dust via SEM images, though the agglomerates themselves were not necessarily a focus of the research (e.g., LaBranche, et al.²⁹, Pandey, et al.³⁰, Su, et al.³¹, Zazouli, et al.³²).

To specifically investigate the formation and relative dispersibility of agglomerates in RCMD, the authors' research team recently conducted laboratory experiments in two stages³³. In the first stage, dust was generated by pulverizing coal and rock materials; sampled passively, without use of a cyclone, tubing, or air pump; and analyzed directly by manual SEM-EDX to classify respirable-sized particulates—i.e., as either independent coal or mineral particles; or agglomerates containing coal, minerals, or both. (Here, 'particulates' are distinguished from 'particles'; whereas 'particle' refers to a single, solid piece of matter, a 'particulate' is an entity made up one or more particles, e.g., an agglomerate.) In the second stage, the dust samples from the first stage were dispersed in deionized water or a simulated human lung surfactant; redeposited; and reanalyzed to evaluate changes in the relative proportions of independent particles versus agglomerates. Results from the first stage indicated a high degree of agglomeration (i.e., between 27–74% of the entities counted were agglomerates rather than independent particles)³³. This provides further evidence that agglomerates in RCMD probably form due to dust generation processes or in the coincident high-concentration environment—and are not simply formed as an artifact of the respirable sampling procedure, which more likely destroys them (per Armbruster²⁸). Additionally, results from the second stage showed some dispersion of agglomerates by mechanical forces, and an enhanced effect in the presence of lung surfactant³³. These findings highlight the complexity agglomerates may present for understanding the nature of real respirable dust exposures, and their possible outcomes.

Moreover, agglomerates may complicate dust particle analysis. As mentioned above, this was the case when attempting to characterize the degree of surface-occluded silica particles in RCMD analyzed directly on the sample filter (i.e., without dispersion)²⁷. Therefore, in the two-stage experiments to study agglomerates specifically, the SEM-EDX analysis combined both EDX elemental mapping and visual inspection of SEM images to identify and classify agglomerates by their constituent particles³³. However, for automated SEM-EDX analysis, agglomerates could challenge particle sizing and classification schemes^{33–35}. To explain: software used for such automated work typically relies on image contrast to identify and size particles, and then uses the EDX data to classify each particle (e.g., see Johann-Essex, et al.³⁶, Keles, et al.³⁷). Depending on the analysis parameters (e.g., resolution, contrast settings), the software might see an agglomerate as a single particle and classify it based on the mixed EDX spectrum contributed by its constituents. Not only could this situation increase the apparent particle size distribution of the sample, but it could also influence the apparent distribution of particle types. For instance, consider a sample with many agglomerates containing silica particles along with aluminosilicates. Such agglomerates could often be classified as single, relatively large aluminosilicate particles. This is because classification criteria for silica particles is typically "exclusive", meaning it is based on the virtual *absence* of elements other than silicon and oxygen (and carbon if the analysis is done on a carbon-rich background); whereas the classification of aluminosilicates is more inclusive since these minerals are more elementally diverse. The net result in this instance is likely to be underestimation of the abundance of silica particles.

Indeed, the potential complications posed by agglomerates for dust analysis are precisely why particles are often dispersed prior to analysis^{25,26}; pre-dispersion and use of pure reference particles are also standard practice in silica toxicity studies^{38,39}. Although these conditions simplify data interpretation, they might neglect the true nature of particles in the exposure environment. In the case of respirable silica-containing agglomerates, specifically, there could be several important implications with respect to: exposure characterization (e.g., how prevalent are respirable silica-containing agglomerates? how can they be measured?); lung response (e.g., are respirable silica-containing agglomerates dispersed upon inhalation or in the lung? how does this affect mobility/toxicity of the contained silica particles?); and dust control (e.g., can agglomeration be enhanced to improve filtration-based controls, or to simply shift dust out of the respirable range?).

To gain further understanding, this study had two objectives: (1) to investigate the effects of agglomeration, in general, on apparent particle size and mineralogy distributions observed in RCMD samples, and (2) to explore the relative agglomeration of silica, specifically, in RCMD. For this, a total of 26 RCMD samples representing 17 underground coal mines were analyzed direct-on-filter and following dispersion, using both automated and manual SEM-EDX methods. Additionally, several passive dust samples were collected in a single mine to

observe the occurrence of respirable silica without any influence of standard RCMD sampling equipment (i.e., air pump, cyclone, and tubing).

Materials and methods

Mine dust samples

A total of 26 respirable coal mine dust (RCMD) samples were used for this study. These were part of a larger inventory of RCMD samples collected by the authors for prior studies (e.g., Sarver, et al.¹⁹, Keles, et al.⁴⁰; since earlier analysis was non-destructive, the samples were still available for the current work. Moreover, it is important to note that selection of samples for this study from the larger inventory was based on two key criteria: First, earlier analysis by automated SEM-EDX indicated that the particulate loading density (PLD) on the sample filters was relatively low (i.e., less than 0.035 #/μm², per Keles, et al.⁴⁰). This was an important condition for ensuring minimal interference (i.e., in particulate identification and sizing, and EDX data collection) between particulates that just happened to deposit nearby to one another on the filter. This sort of interference is fundamentally different from that caused by agglomerates, with the former being an artifact of the sampling process and the latter more likely a product of dust generation in the mine atmosphere. The second criterion for sample selection was that earlier SEM-EDX work also indicated the samples contained at least 2% silica (by number percentage)⁴⁰. This was important considering the research objective to explore the relative agglomeration of silica in RCMD.

The 26 RCMD samples used for this study had been collected in 13 active underground coal mines (see Table S1 in Supplemental Information). These were “stationary” samples, meaning they were collected in a static location rather than on a person. Each sample was collected in one of five standardized locations: intake (I), bolter (B), feeder (F), production (P), and return (R). For the purposes of this study, samples are labeled by their respective mine and sampling location (e.g., sample “10-B” was collected in Mine 10 in the B location). It is important to note that two P samples (15-P and 25-P, which were collected in Mines 15 and 25, respectively) were collected under normal production conditions; meaning the continuous miner was cutting the entire height of the entry during the sampling period, and the samples were collected just downwind of the miner. For the other three P samples (collected in Mine 27), the sampling location was the same but the miner cutting conditions were unique; the miner was targeting only the coal seam during collection of two samples (27-Pcoal1 and 27-Pcoal2), and the miner was targeting only the roof rock during collection of the other sample (27-Prock). All 26 RCMD samples were collected directly onto 37-mm polycarbonate filters (PC, track etched with 0.4 μm pore size) housed in closed cassettes. The samples were collected using standard sampling trains for US coal mines (i.e., 10-mm nylon cyclone and air pump operated at 2 L/min). Sampling inlets were positioned at approximately “head height” (i.e., about 1.8–2.0 m from the mine floor) and mid-width of the sampled air way.

In Mine 27, a total of four passive dust samples were additionally collected (labeled as, e.g., “27-Pass1”). The passive sampling duration overlapped with the RCMD sampling durations in this mine, with the passive samplers set up in the same location as the RCMD samplers (i.e., in the P location, just downwind the active continuous miner). However, while the RCMD samples correspond to the miner targeting a particular stratum in the entry (i.e., either the coal or the roof rock, over relatively short time periods), the passive samples were collected during the entire cutting period (i.e., they contain particulates generated from cutting both the coal and rock strata). The passive samples were collected using a special apparatus (i.e., the UNC Passive Aerosol Sampler per Ott and Peters⁴¹). Essentially, the apparatus consists of a particulate deposition substrate that is placed within a shelter during sampling. For this study, the substrate was a 10-mm section of PC filter (i.e., identical material to that used for the RCMD sampling), which was pre-mounted with adhesive onto an aluminum SEM stub. For sampling, a mesh cap is placed over the filter stub, and the assembly is placed inside a shelter with open sides. The cap and shelter are designed to limit deposition of relatively large particles (i.e. >125 μm) but allow passive deposition of smaller particles.

Sample Preparation

For the RCMD samples, each original 37-mm PC filter was used to create a pair of 9-mm filters for SEM-EDX analysis (Fig. 1). The first was used for “direct”-on-filter analysis and was created by simply taking a 9-mm subsection from the original filter. The second was used for “recovered” dust analysis and was created by recovering and redepositing dust from about one quarter of the original filter. For this, the quarter section was placed into a clean glass tube, submerged in isopropyl alcohol (IPA), and sonicated for 3 min to recover the dust from the filter; per Gonzalez, et al.³³ and Greth, et al.⁴², this procedure is expected to promote dispersion of agglomerates. The resultant suspension was then pulled through a new 47-mm PC filter (again, track etched with 0.4 μm pore size) using a vacuum filtration unit to redeposit the dust. After the new filter was allowed to dry completely, a 9-mm subsection was cut for SEM-EDX analysis. All the direct and recovered 9-mm filters were prepared for SEM-EDX analysis by mounting on an aluminum stub and sputter coating with a thin layer of Au/Pd.

For the passive dust samples, the mesh cap was simply removed from the filter stub, and then these samples were sputter coated for SEM-EDX analysis. No attempt was made to create recovered filters from the passive samples; since the dust collection substrate is already quite small and was pre-mounted to the aluminum stub with adhesive, any attempt to recover the dust might have resulted in substantial sample loss or contamination.

SEM-EDX analysis

SEM-EDX work was done with an FEI Quanta 600 FEG environmental SEM (Hillsboro, OR, USA) equipped with a secondary (SE) and backscatter electron (BSE) detectors and a Bruker Quantax 400 EDX spectroscope (Ewing, NJ, USA). For each of the direct and recovered filters prepared from the RCMD samples, analysis was completed using two methods: (1) an automated method was used to estimate particulate mineralogy and size

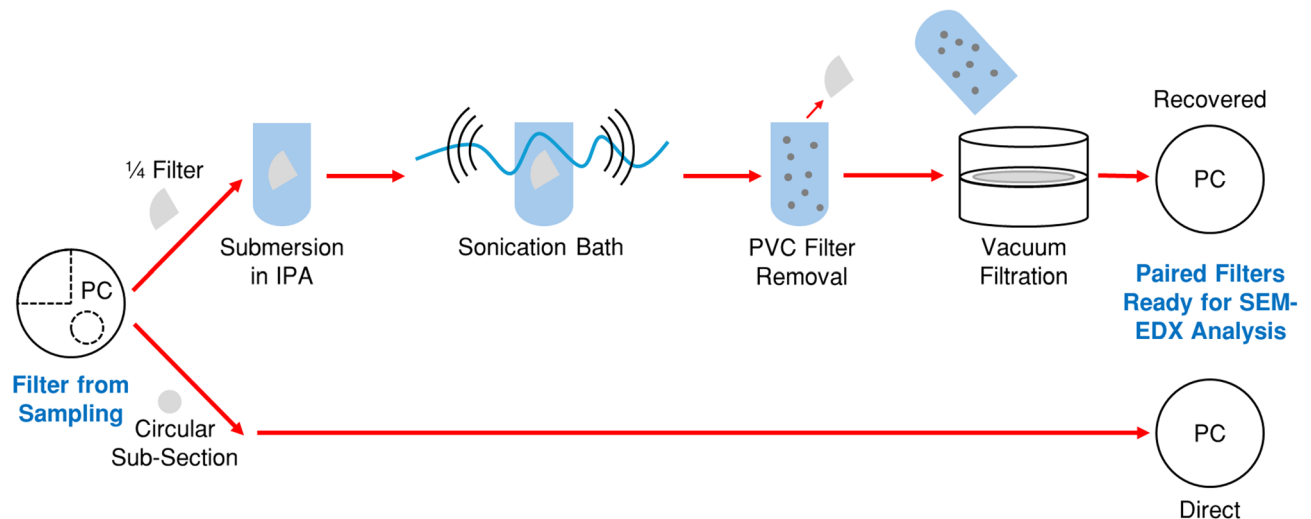


Fig. 1. Procedure to prepare direct and recovered filter pairs from each of the 26 RCMD samples.

distributions, and (2) a manual method was used to characterize respirable silica-containing particulates based on their constituents. For the passive dust samples, only the manual SEM-EDX analysis was completed.

The automated SEM-EDX method used here is the “supramicron” method presented in Sarver et al.¹⁹. Briefly, it consists of a routine programmed in Bruker’s Esprit software (Version 1.9) to identify and analyze particulates in the range of 1–10 μm in length. (Notably, the routine relies on contrast in the BSE images to identify dust on the PC filter background, but this does not enable discrimination between independent particles and agglomerates. Thus, while other reports of work with this and similar routines typically present results for “particles”, here the term “particulate” is used to deliberately acknowledge that some entities identified by the routine may not be independent particles.) The automated routine moves across the filter sample collecting data in pre-programmed fields (1 mm spacing, field area of 14,025 μm^2 at 1000 \times magnification); it is set to collect data on a maximum of 50 particulates per field, targeting at least 500 particulates per filter (i.e., minimum of 10 fields). The length and width of each particulate are recorded, as are the normalized atomic percentages of eight elements (carbon, oxygen, aluminum, silicon, calcium, magnesium, iron, and titanium) based on the EDX spectrum. Then, the elemental data is used to bin each particulate into one of seven inferred mineralogy classes: carbonaceous (C), mixed carbonaceous (MC), aluminosilicates (AS), silica (S), other silicates (OS), carbonates (CB), or heavy minerals (HM). C and MC are typically interpreted as coal dust, and HM includes iron and titanium oxides or sulfides. An others class (O) is used for particulates not classified into one of the defined classes. Using the data generated by the automated SEM-EDX method, the particulate mineralogy and size distributions were estimated for each of the direct and recovered RCMD filters. As a general measure of size distribution on each filter, the D_{50} value was computed (i.e., the median particulate length). The PLD on each filter was estimated as the number of particulates identified per analyzed area ($\#/\mu\text{m}^2$).

Following the automated SEM-EDX analysis, a manual method was also used to investigate respirable silica-containing particulates (i.e., 1–10 μm in length) on all the direct and recovered filters created from the original RCMD samples. For this, a similar approach to that established by Gonzalez, et al.³³ was used. Briefly, using the same grid spacing as for the automated method, manual work proceeded field-by-field to first identify and then characterize respirable silica-containing particulates. In each field, both an SE image and elemental map were captured at 5 kV and 4000 \times magnification; the map only included silicon and aluminum. To identify silica-containing particulates, areas rich in silicon but with minimal aluminum content were interpreted as silica, and areas with both silicon and aluminum content were interpreted as aluminosilicates. (Notably, this approach was based on substantial experience by the authors using SEM-EDX to analyze RCMD samples, which has shown that respirable silica and aluminosilicates are generally the only major types of silicon-rich minerals^{9,19,36,43,44}. Based on visual analysis of both the elemental map and SE image in each field, the identified silica-containing particulates were binned into one of five categories per Fig. 2: independent silica particles (S), silica and other mineral agglomerates together (S+OM), silica and coal particles together (S+C), silica, other minerals, and coal particles together (S+OM+C), and two or more silica particles together (S+S). This work proceeded until a total of 21 fields had been analyzed (see Figure S1 in the Supplemental Information for layout of fields.) Importantly, all the manual SEM-EDX work was done by a single, experienced analyst to limit bias in particulate identification and characterization.

Results and discussion

Effects of agglomeration on particulate characterization

Results of the automated SEM-EDX analysis on each of the direct and recovered filter pairs derived from the 26 RCMD samples are tabulated in the Supplemental Information (Table S2). For each filter, data is presented for

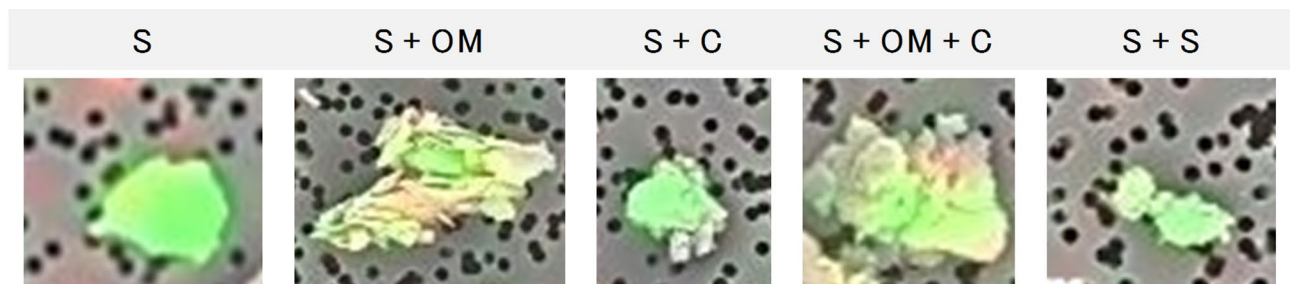


Fig. 2. Example particulates in each category used for silica-containing particulates characterization. (S=independent silica particle, S + OM=silica and other minerals agglomerates together, S + C=silica and coal particles together, S + OM + C=silica, other minerals, and coal particles together, S + S=two or more silica particles together.)

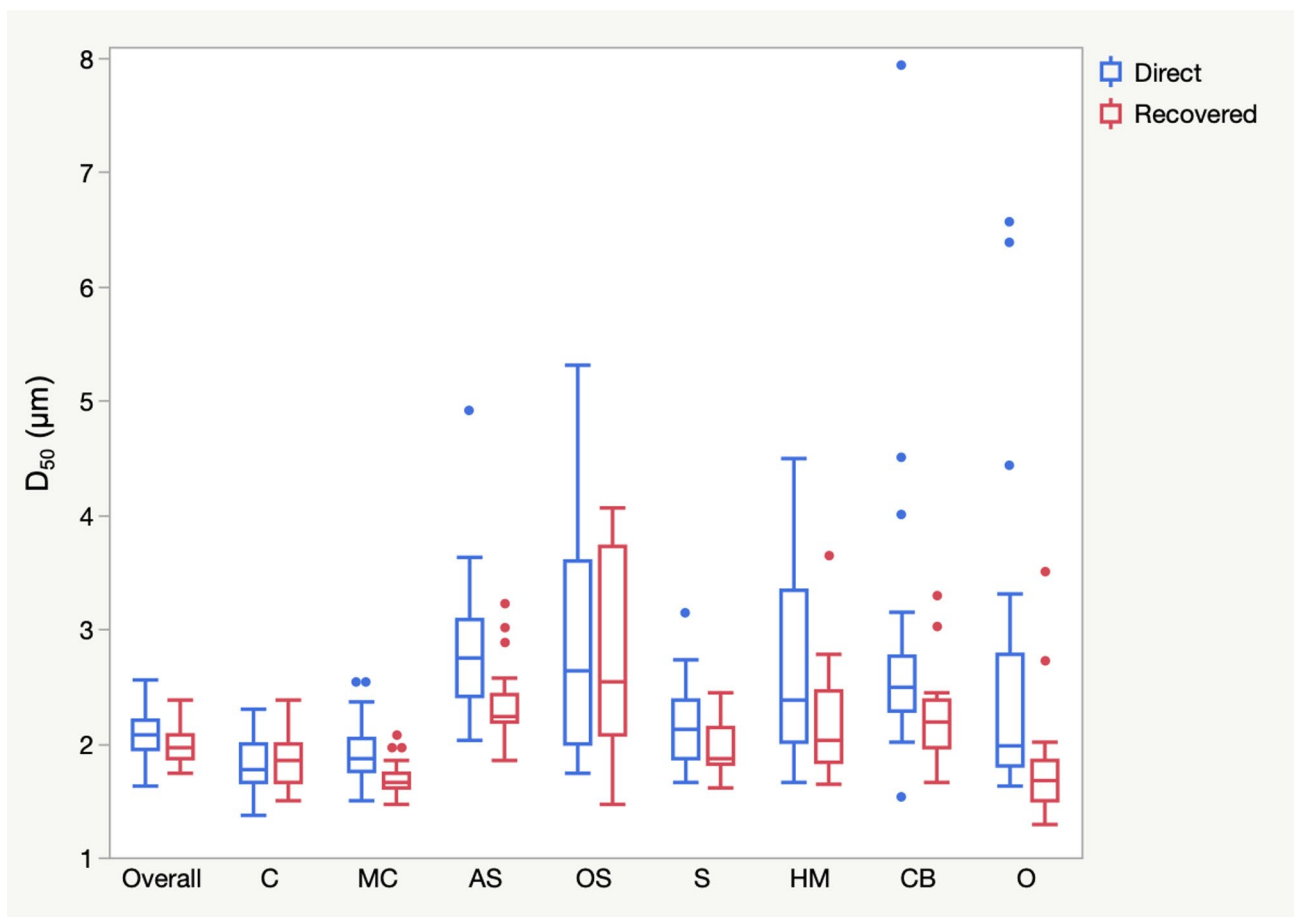


Fig. 3. Distribution of particle length (expressed as D_{50}) observed from the automated SEM-EDX analysis on direct versus recovered filters prepared from the 26 RCMD samples. Results are shown by each mineralogy class and overall (i.e., all particulates analyzed on a filter).

mineralogy distributions (number percentage by class) and D_{50} values (per mineralogy class and for all particles analyzed on the filter) are presented as a general measure of particulate size distributions.

Figure 3 shows box and whisker plots for the D_{50} values determined for the direct and recovered filters. (Notably, the OS, HM, and O classes have the widest boxes and whisker because they have relatively low particulate counts compared to the other classes, e.g., typically less than 1% per Supplemental Table S2.) With the exception of the C class results, the particulate sizes on the recovered RCMD filters appear to be somewhat finer than on the direct filters. And, based on a paired t-test ($\alpha = 0.05$), the difference in observed D_{50} values for the MC, AS, S, HM, CB, and O classes are statistically significant (see Supplemental Table S3 for P values). This apparent shift in the size distribution is consistent with dispersion of agglomerates during the dust recovery

procedure. That said, there could be other contributing factors. For example, coarse dust particles could be more susceptible to loss during dust recovery and redeposition procedures, or the relative particle size distributions could have differed between the filter subsections that were prepared for the direct versus recovered dust analysis (e.g., based on deposition pattern on the original PC filter).

Assuming that dispersion of agglomerates is the primary explanation for the results shown in Fig. 3, classes with greater observed change in the size distribution between direct and recovered filters are more likely to be dominant with respect to mineralogy classification. Case in point, the AS class exhibits the most change between the direct and recovered filters. This is consistent with the idea that agglomerates containing AS particles are likely to be classified as AS—even if they also contain other types of particles—because the AS classification is elementally “inclusive” (i.e., allowing for silicon, aluminum, iron, etc.) to catch most AS minerals that commonly occur in RCMD. In essence, this means that AS-containing agglomerates might “hide” their other constituent particles, including some S particles. While the S class does exhibit a shift toward finer particulates on the recovered filters, the change is less substantial than that for the AS class. This could mean that respirable silica-containing agglomerates on the direct filters are only sometimes classified as S particulates. For instance, the S + S and S + C agglomerate types shown in Fig. 2 are likely to be classified S particulates by the automated analysis, since the S class allows for silicon, carbon and oxygen. However, the S + OM and S + OM + C types might only be classified as S particulates under limited circumstances (e.g., if the contained S particle(s) are relatively coarse or centrally located, as to dominate the EDX spectrum, compared to the other particles contained in the agglomerate). On the other hand, the observation of minimal change in particulate size for the C class in Fig. 3 suggests these particulates are most often independent particles (probably coal dust). Like silica, if coal particles do occur in agglomerates, they are likely to be hidden by the other constituent particles (i.e., because the classification criteria for the C class are elementally exclusive).

To gain more insights, Fig. 4 presents the mineralogy distribution results derived from the automated SEM-EDX method for the RCMD samples. The figure shows the relative abundance of particulates in each mineralogy class for the direct filters (Fig. 4a), the recovered filters (Fig. 4b), and then for the *difference* between the direct and recovered filter in each pair (Fig. 4c). (For the difference plot, positive values for a given class indicate the direct filter had a greater relative abundance of particulates in that class than the recovered filter, and vice versa). A paired t-test was used to compare the mean number percentage in each class between the direct and recovered filters (P values in Supplemental Table S3), but only the HM class exhibited a significant difference ($P=0.001$). While the HM class represents relatively small percentages of the total particulates, HM particulates were more abundant on the recovered filters. This might mean that HM particles were frequently hidden within in agglomerates on the direct filters.

To explore other possible effects of agglomerates on particulate classification, it is helpful to group the samples with respect to the differences observed between the direct and recovered filter in each pair (i.e., per Fig. 4c). For eight of the 26 filter pairs (left side of the plot), the difference between the direct and recovered filter results were within 10% for each mineralogy class—in other words, the direct and recovered filters had relatively similar mineralogy distributions. These results suggest the direct filters contained relatively few agglomerates (or that the agglomerates did not disperse during the recovery procedure.)

However, for the other 18 filter pairs (right side of Fig. 4c plot), the difference between the direct and recovered results was greater than 10% for at least one mineralogy class—and the largest differences were typically observed for the AS and C classes. For 12 of these pairs, the direct filters appeared to contain more C (and typically more MC) particulates, whereas recovered filters contained more AS (and typically more S) particulates. These trends are logical in view of the particle size results and consistent with the related discussion points above. For example, large increases in the relative abundance of AS particulates on recovered filters (versus their direct counterparts) fits with the idea that agglomerates are often dominated by AS particles and were dispersed during the recovery procedure. Likewise, frequent (albeit smaller) increases in the relative abundance of S particulates on recovered filters supports the notion that S particles can be hidden within agglomerates prior to dispersion. On the other hand, the decrease in relative abundance of C particulates on the recovered filters supports the idea that coal dust may often occur as independent particles rather than within agglomerates.

For another five of the filter pairs with greater than 10% difference between the direct and recovered results for at least one mineralogy class, the direct filter appeared to contain more AS particulates, whereas the recovered filter contained more C particulates. Unlike most other samples, the coal dust particles in these samples might have more frequently been part of agglomerates on the direct filters—but essentially hidden by the other constituents (commonly AS particles) during the automated SEM-EDX analysis. (For sample 11-R, it is also worth noting that the direct filter PLD [0.034 particulates/ μm^2] was close to the threshold used to screen samples for inclusion in this study [0.035 particulates/ μm^2]. Higher PLD can cause interference between particulates, so it is possible that the very high AS content observed for the 11-R direct filter is partially related to PLD.)

The final filter pair that exhibited a greater than 10% difference in at least one mineralogy class was from sample 17-B (far right side of Fig. 4c plot). It appeared to have lower abundance of CB particulates on the direct filter (versus the recovered filter), balanced by slightly lower abundance of particulates in most other classes. This suggests that CB particles on the direct filter were sometimes agglomerated with (and obscured by) a variety of other particles.

To check for trends in mineralogy distributions related to specific sampling locations, Tukey-Kramer HSD pairwise tests ($\alpha=0.05$) were performed using each of the datasets presented in Fig. 4. However, no statistical differences were found (P values in Supplemental Table S4). (Note that P samples from Mine 27 were not included in statistical tests since these samples represented different dust generating conditions than the other P samples per above.) Previous studies, including Sarver, et al.⁹ and Sarver, et al.¹⁹, have found significant differences in RCMD mineralogy distributions depending on sampling location. Lack of location-specific trends here could

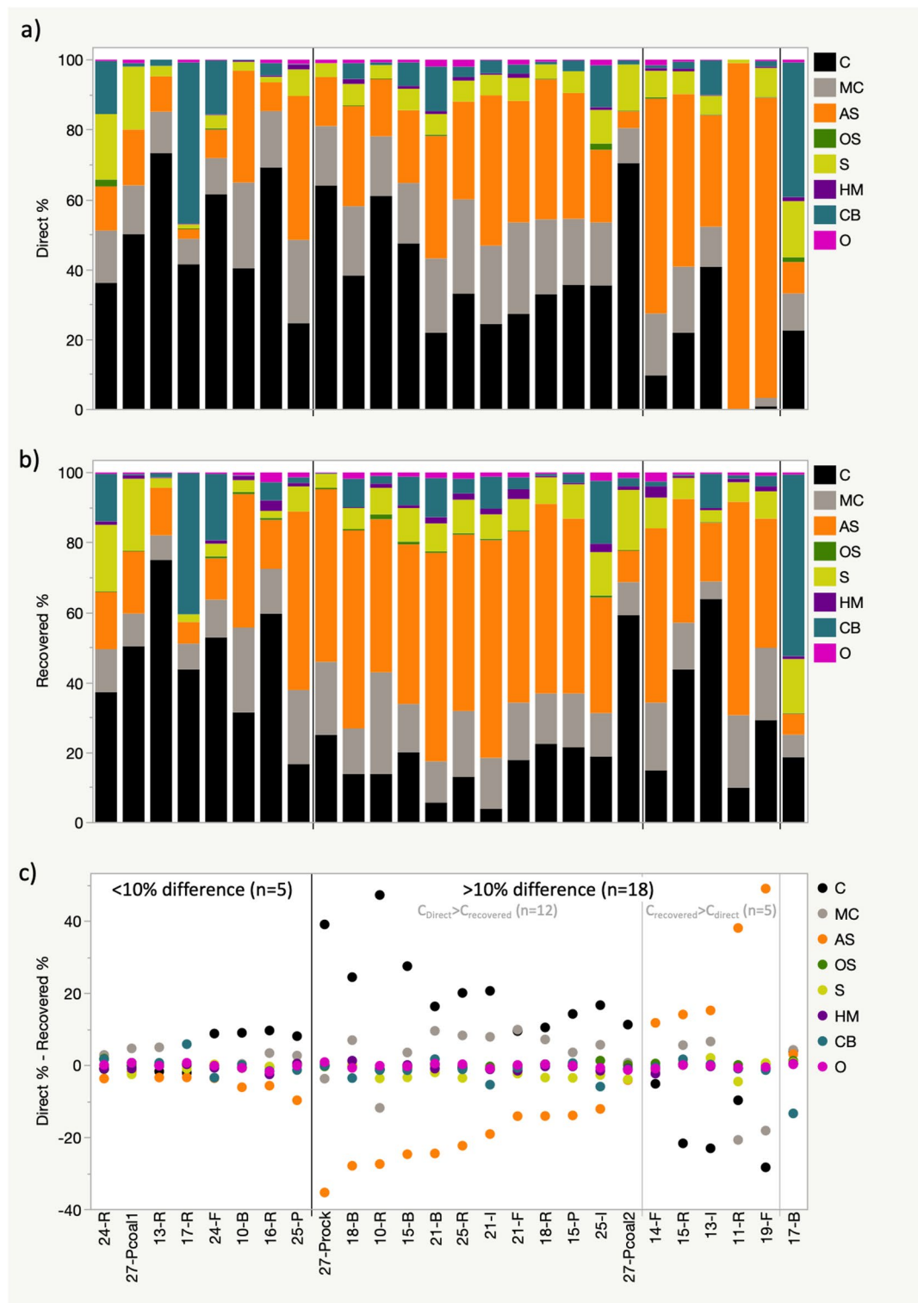


Fig. 4. Mineralogy distribution results derived from the automated SEM-EDX analysis on (a) direct and (b) recovered filters prepared from the 26 RCMD samples. Plot c) shows the difference in results between the direct and recovered filters (i.e., difference between plots a) and (b) values). Samples are ordered by the relative difference between direct and recovered filter results: samples with <10% difference ($n=8$) in any mineralogy class are on the left, and samples with >10% ($n=18$) in at least one class are on the right; within the >10% group, $n=12$ samples show higher C and lower AS abundance on the direct filter, $n=5$ samples show lower C and higher AS abundance on the direct filter, and $n=1$ sample shows lower CB abundance on the direct filter.

simply be due to the relatively small number of samples for each location and/or the fact that different mines are represented for each location (e.g., the F location includes samples from Mines 14, 19, 21 and 24, whereas the I location includes samples from Mines 13, 21 and 25).

Relative abundance and dispersibility of silica-containing agglomerates in RCMD

The manual SEM-EDX analysis to investigate silica-containing particulates, specifically, was conducted on each of the direct and recovered filter pairs derived from the 26 RCMD samples, as well as the four passive samples. As explained earlier, for this, all silica-containing particulates that were identified in the manual SEM-EDX analysis were binned into one of the five categories exemplified in Fig. 2. Results are given in Supplemental Table S5 (as number percentage by category) and plotted Fig. 5. Again, plots are presented for the direct filters (Fig. 5a), the recovered filters (Fig. 5b), and then for the difference between the direct and recovered filter in each pair (Fig. 5c).

From Fig. 5, several key observations can be made. First, on the filters analyzed directly, the majority of silica particles (in the size range investigated here) are contained in multi-particle clusters—presumably agglomerates. Considering all 26 direct filters, independent silica particles were observed to account for between 0 and 43% of all silica-containing particulates, with a mean value of just 23%. Results showed that silica was most often clustered with other minerals, predominantly aluminosilicates, with the S + OM category accounting for 7–68% (mean of 40%). In some samples, clusters containing coal dust particles were also abundant; S + C particulates accounted for 2–37% (mean of 16%) and S + OM + C particulates accounted for 2–57% (mean of 15%). Less often, clusters were observed that only contained silica particles, with the S + S category accounting for 1–21% (mean of 7%).

Compared to distribution of silica-containing particulates on the direct filters, Fig. 5 shows a consistent tendency toward a higher relative abundance of independent silica particles on the recovered filters (33–67%, mean of 47%). This is evident in 25 of the 26 filter pairs, and it validates the automated SEM-EDX results which suggest dispersion of silica-containing agglomerates via the sample recovery and redeposition procedure used here. From Fig. 5, some understanding can also be gained regarding the *types* of agglomerates most prone to dispersion. On the recovered filters, the S + OM and S + OM + C categories accounted for just 3–36% (mean of 23%) and 0–18% (mean of 7%), respectively, of all silica-containing particulates. Compared to the results for the direct filters, Fig. 5c illustrates that these results represent a substantial increase in the relative abundance of S and decrease in the abundance of S + OM and S + OM + C; and paired t-tests showed that the differences were statistically significant (P values in Supplemental Table S6). On the other hand, significant differences between the direct and recovered filters were not observed for the S + S and the S + C categories. Figure 5 shows that changes in S + S relative abundance were typically minimal. While more substantial changes in the S + C abundance were observed, they were somewhat inconsistent with 15 filter pairs showing more S + C particulates on the direct filters, and 11 pairs showing the opposite trend.

Collectively, the results of the manual SEM-EDX analysis indicate that silica particles in RCMD samples can frequently occur as agglomerates. Further, at least for the mines and sampling locations represented here, agglomerates containing silica and other minerals (rather than silica and coal, or only silica) are most common—and most easily dispersed. The types of silica-containing agglomerates observed here are likely a product of the primary silica sources and dust generating activities represented by the RCMD samples included in this study. In most of the mines, the roof rock being cut along with the coal seam or drilled for roof bolting is expected to be the main source of silica dust; and the rock strata were typically shale or a mix of shale and sandstone, which undoubtedly also contributed aluminosilicate dust. Further, continuous mining methods (including with a miner or longwall) tend to generate more respirable dust from rock than coal⁴⁵. Thus, it is unsurprising that silica particles might agglomerate more frequently with minerals such as aluminosilicates, rather than coal dust particles, if the process is driven at least partially by the high concentration of particles near the dust-generating activities. Notably, the two samples with the lowest relative abundance of S + OM particulates were the P samples collected in Mine 27 when the miner was targeting the coal seam (i.e., minimal cutting in roof rock). Additionally, the finding that silica particles may be more readily dispersed from other minerals (commonly aluminosilicates) than from coal dust could be related to particle surface and physiochemical characteristics. A number of factors contribute to particle adhesion including particle charge, pore structure, and macromolecules^{46,47}.

To explore possible trends in the distribution of silica-containing particulates with respect to sampling location, Tukey-Kramer HSD pairwise tests were again conducted on each of the datasets presented in Fig. 5. (Again, the P samples from Mine 27 were excluded from this analysis.) No significant differences were found between locations for the results on the direct filters, however differences were found between the B and I locations and the B and F locations for the S + S particulates (P values in Supplemental Table S7). This, in combination with the difference in S + S abundances shown in Fig. 5c, suggests that silica-only agglomerates generated by the roof bolter may be less dispersible than their counterparts generated by other processes (e.g., crushing of rock material in the feeder breaker).

The observation of relatively less dispersible (i.e., more persistent) particulate types—i.e., including some S + S and S + C particulates—raises the possibility that some such entities are actually *aggregates* rather than agglomerates. Whereas agglomerates might be formed by coagulation of independent particles in a high concentration environment and held together by relatively weak surface forces, aggregates might be inherent to the source rock from which the dust was generated and held together by stronger forces (e.g., cementation). Unfortunately, a clear distinction cannot be made in the current study between agglomerates and aggregates, but could be explored with additional experiments (e.g., applying successive dispersion steps).

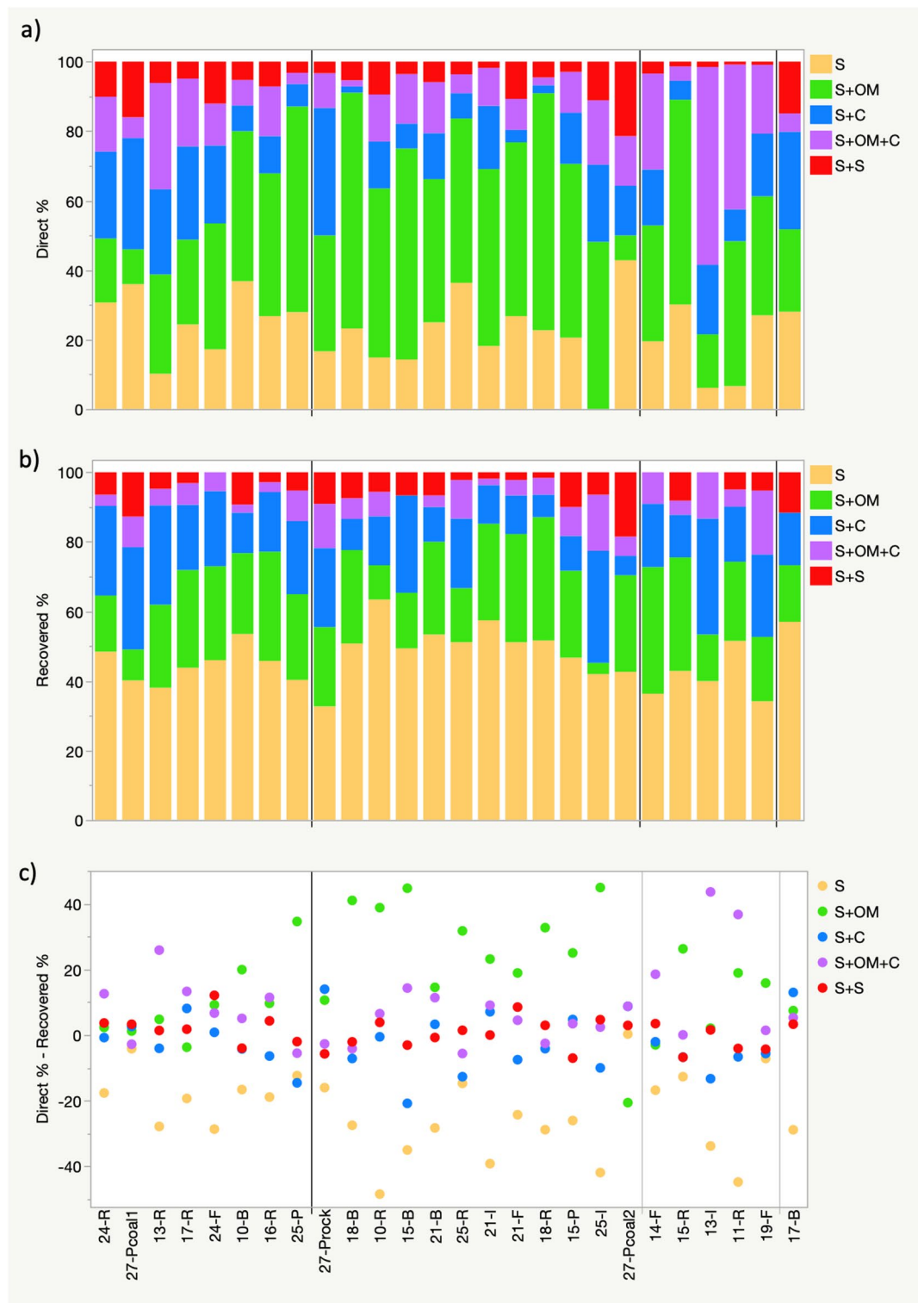


Fig. 5. Distribution of silica-containing particulates observed from the manual SEM-EDX analysis on (a) direct and (b) recovered filters prepared from the 26 RCMD samples. Plot (c) shows the difference in results between the direct and recovered filters (i.e., difference between plots a) and b) values). Samples are presented in the same order as in Fig. 4.

Relative abundance of respirable silica-containing agglomerates in passive samples

As stated, four passive dust samples were collected in Mine 27 and analyzed manually by SEM-EDX. Example images (SE micrographs and corresponding elemental maps to visualize silicon and aluminum content) are presented in (Fig. 6). Based on both the morphology and chemistry, these images clearly demonstrate that

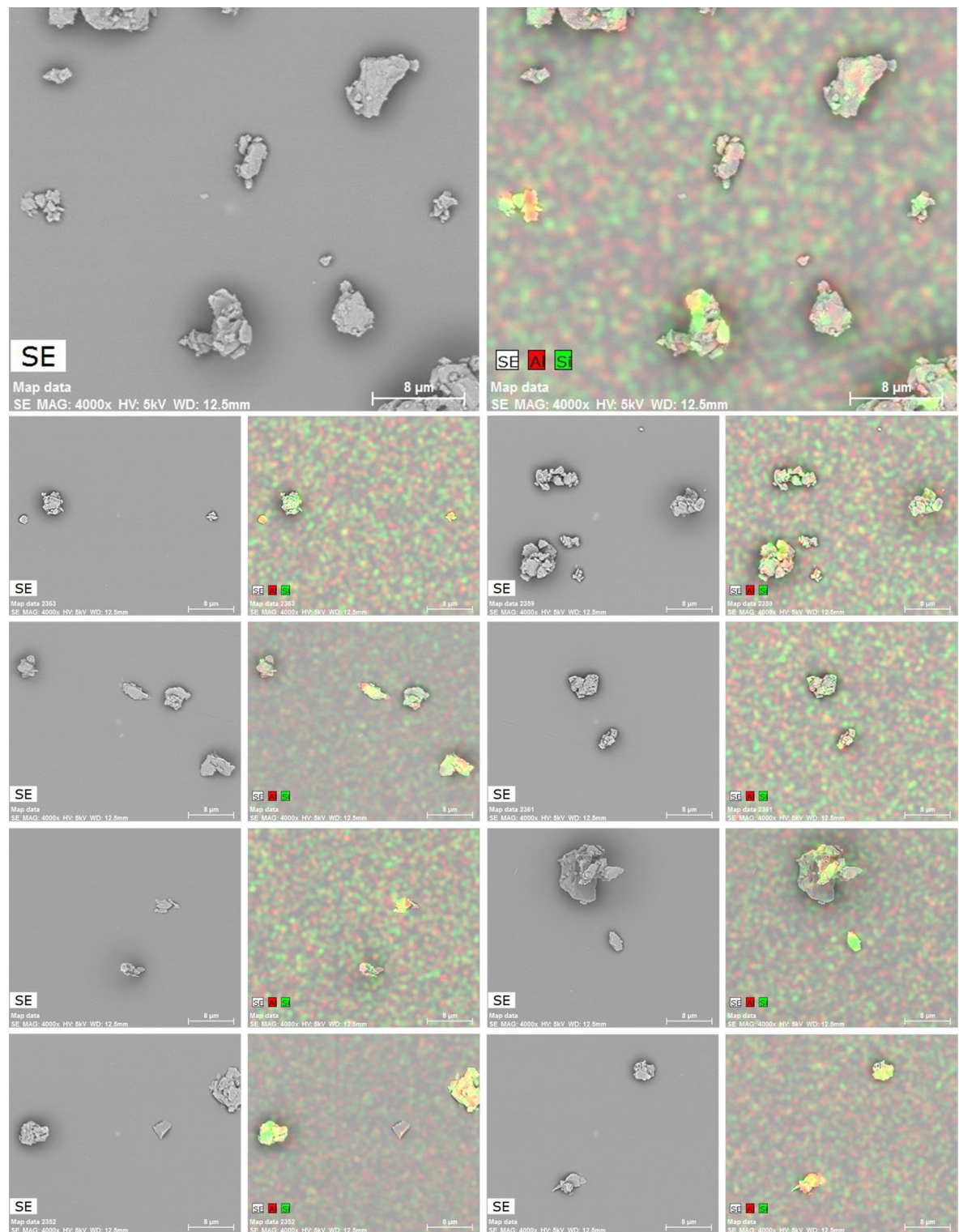


Fig. 6. SEM-EDX images (SE micrographs and corresponding Si and Al maps) exemplifying silica-containing agglomerates observed in passive samples from Mine 27.

respirable-sized agglomerates do occur in the coal mine atmosphere—and can contain silica particles. This is an important finding because it confirms that such agglomerates are not merely an artifact of typical respirable dust sampling procedures, which utilize apparatuses that include tubing and size separators (e.g., cyclones) that could influence formation (or dispersion) of agglomerates.

The results of the particulate characterization analysis on the passive samples are shown in Fig. 7 (data in Supplemental Table S5) alongside the results for the RCMD samples from Mine 27 that were obtained on

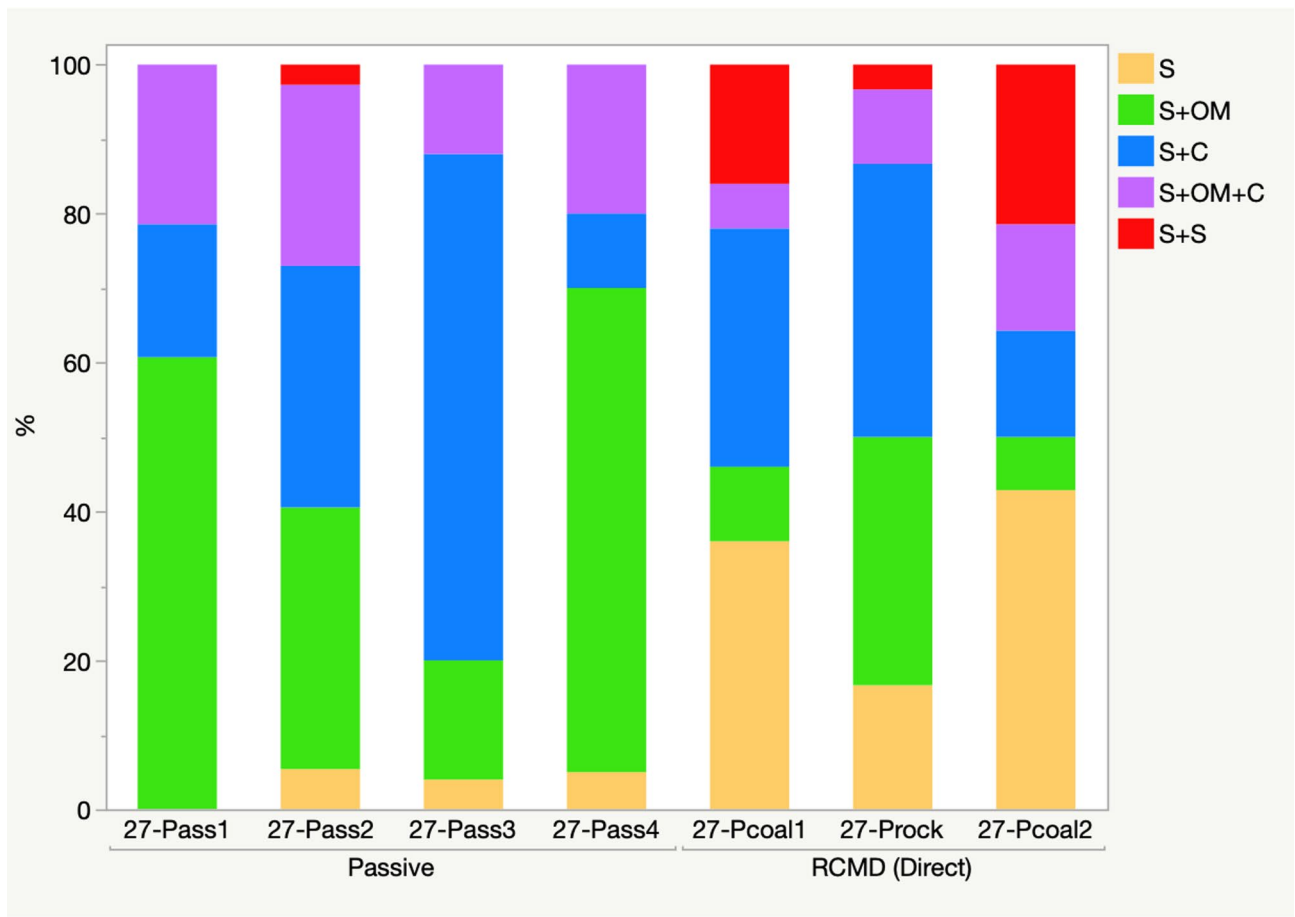


Fig. 7. Distribution of silica-containing particulates observed from the manual SEM-EDX analysis on passive dust samples and RCMD samples collected in Mine 27. (For the RCMD samples, results represent analysis directly on the sample filter.)

the directly-analyzed filters. It is reiterated that the passive samples represent dust collected in the Mine 27-P location over a relatively long total duration, during which the miner was alternating between cuts targeting primarily coal or primarily roof rock; whereas the RCMD samples were collected over relatively short periods within that same duration, with the shorter periods corresponding to a specific miner cut targeting either coal or roof rock. While some general comparisons can be made between these particular passive and RCMD samples, no statistical tests were conducted.

The most striking observation from Fig. 7 is the very low relative abundance of independent silica particles on the passive samples (5% or less in the S category), countered by the very high abundance of silica-containing agglomerates (95% or more within all agglomerates categories). Comparatively, the RCMD samples had more independent silica particles and fewer agglomerates. These results suggest that respirable-sized agglomerates are susceptible to dispersion during sampling with a cyclone size-selector, consistent with predictions by Armbruster²⁸. This could have important implications for evaluating exposures, since it implies that RCMD particulates as sampled could be fundamentally different than RCMD particulates as inhaled. Obviously, additional research is needed to assess the dispersibility of agglomerates upon inhalation—and the possible effects on exposure outcomes.

The data in Fig. 7 further shows that, of the particulates in the agglomerate categories, the passive samples tended to have more S + OM particulates than the RCMD samples, whereas the RCMD samples tended to have more S + S particulates. (Differences between the relative proportions of S + C and S + OM + C particulates are more nuanced.) These results are consistent with inferences from the automated SEM-EDX results in terms of suggesting that agglomerates of silica and other minerals might be more readily dispersed than agglomerates of silica and coal—and agglomerates of only silica might be relatively persistent.

Conclusions

Respirable dust exposure monitoring and control has conventionally relied on mass-based measures, but there is a growing recognition that particulate-level data is needed to fully understand, and ultimately prevent, health effects. In the context of coal mines and other occupational environments, characterization of respirable silica is especially important. Although it is convenient to model silica and other dust based on an assumption of

high purity and independent particles, reality is more complicated. Prior studies have indicated agglomerates in respirable coal mine dust, and the passive samples collected and analyzed for this study (albeit from just a single mine) clearly demonstrate that agglomerates can occur as such in the mine atmosphere. Depending on the characteristics of the agglomerates themselves (e.g., size, included particles, relative dispersibility), they could have important implications for health, and therefore it could be important to capture them in dust sampling and analysis. Notably, the dust samples included in this study were stationary samples, and therefore the results cannot be directly related to personal exposures.

With respect to sampling, the results of this study suggest that respirable sized agglomerates are susceptible to dispersion. Indeed, some appeared to be broken up by the typical respirable sampling procedure, and others appeared to be broken up by a sample preparation procedure that included sonication in isopropyl alcohol. Overall, agglomerates containing minerals (including silica) appeared to disperse more easily than agglomerates containing minerals and coal. This might be related to surface properties of different particle types, though presence of aggregates (in addition to agglomerates) cannot be ruled out.

With respect to particulate analysis, SEM-EDX is a powerful tool because it can provide both size and elemental data. However, the presence of agglomerates can influence apparent particle size and mineralogy distributions when using an automated method like the one used in this study (i.e., each particulate is assumed to be an independent particle). In the case of respirable silica in coal mine dust, abundant agglomerates may have the effect to “hide” the silica particles with such a method. To better characterize agglomerates, a method that enables differentiation between the constituent particles is needed. This was accomplished in the current study using manual analysis, but might also be accomplished using advanced SEM-EDX tools (e.g., with capabilities for grain boundary analysis).

The above points can inform particulate sample collection, preparation, and characterization efforts. For example, if an objective is to evaluate the size distribution and mineralogy of independent particles, traditional respirable sampling with adequate dust dispersion prior to analysis may be appropriate. On the other hand, if the objective is to characterize particulates as they actually occur in the exposure environment, alternate sampling techniques—including passive sampling—and advanced particulate analysis may be required.

Data availability

All data is available in the article, Supplemental Information or upon reasonable request to the corresponding author.

Received: 28 May 2024; Accepted: 8 May 2025

Published online: 20 May 2025

References

- Occupational Exposure to Respirable Crystalline Silica—Review of Health Effects Literature and Preliminary Quantitative Risk Assessment. edited by Occupational Safety and Health Administration (OSHA). Washington, DC, USA: OSHA, (2010).
- Castranova, V. & Vallyathan, V. Silicosis and coal workers' pneumoconiosis. *Environ. Health Perspect.* **108**, 675–684. <https://doi.org/10.1289/ehp.00108s4675> (2000).
- Cunningham, J. G. S. I. L. I. C. O. S. I. S. *Can. Med. Assoc. J.* **30**, 176–179 (1934).
- King, E. J., Mohanty, G. P., Harrison, C. V. & Nagelschmidt, G. The action of different forms of pure silica on the lungs of rats. *Br. J. Ind. Med.* **10**, 9–17. <https://doi.org/10.1136/oem.10.1.9> (1953).
- Leung, C. C., Yu, I. T. S. & Chen, W. *Silicosis Lancet* **379**, 2008–2018, doi:[https://doi.org/10.1016/S0140-6736\(12\)60235-9](https://doi.org/10.1016/S0140-6736(12)60235-9) (2012).
- Rosenman, K. D., Reilly, M. J., Kalinowski, D. J. & Watt, F. C. Silicosis in the 1990s. *Chest* **111**, 779–786. <https://doi.org/10.1378/chest.111.3.779> (1997).
- Trasko, V. M. Silicosis, a continuing problem. *Public. Health Rep.* (1896). **73**, 839–846 (1958).
- Silica, S. & Silicates Coal dust and Para-Aramid fibrils. *IARC Monogr. Eval. Carcinog. Risks Hum.* **68**, 1–475 (1997).
- Sarver, E., Keles, C. & Rezaee, M. Beyond conventional metrics: comprehensive characterization of respirable coal mine dust. *Int. J. Coal Geol.* **207**, 84–95. <https://doi.org/10.1016/j.coal.2019.03.015> (2019).
- Petsonk, E. L., Rose, C. & Cohen, R. Coal mine dust lung disease. New lessons from an old exposure. *Am. J. Respir. Crit Care Med.* **187**, 1178–1185. <https://doi.org/10.1164/rccm.201301-0042CI> (2013).
- Cohen, R. A. et al. Lung pathology in U.S. Coal workers with rapidly progressive pneumoconiosis implicates silica and silicates. *Am. J. Respir. Crit Care Med.* **193**, 673–680. <https://doi.org/10.1164/rccm.201505-1014OC> (2016).
- National Academies of Sciences, E. & Medicine. *Monitoring and Sampling Approaches To Assess Underground Coal Mine Dust Exposures* (National Academies, 2018).
- Agioutanti, E., Keles, C. & Sarver, E. A thermogravimetric analysis application to determine coal, carbonate, and non-carbonate minerals mass fractions in respirable mine dust. *J. Occup. Environ. Hyg.* **17**, 47–58. <https://doi.org/10.1080/15459624.2019.1695057> (2020).
- Doney, B. C. et al. Respirable coal mine dust in underground mines, united States, 1982–2017. *Am. J. Ind. Med.* **62**, 478–485. <https://doi.org/10.1002/ajim.22974> (2019).
- Alnberg, K. S. et al. Progressive massive fibrosis resurgence identified in U.S. Coal miners filing for black lung benefits, 1970–2016. *Ann. Am. Thorac. Soc.* **15**, 1420–1426. <https://doi.org/10.1513/AnnalsATS.201804-261OC> (2018).
- Hall, N. B., Blackley, D. J., Halldin, C. N. & Laney, A. S. Current review of pneumoconiosis among US coal miners. *Curr. Environ. Health Rep.* **6**, 137–147. <https://doi.org/10.1007/s40572-019-00237-5> (2019).
- Mischler, S. E. et al. Differential activation of RAW 264.7 macrophages by size-segregated crystalline silica. *J. Occup. Med. Toxicol.* **11**, 57. <https://doi.org/10.1186/s12995-016-0145-2> (2016).
- Thomas, R. J. Particle size and pathogenicity in the respiratory tract. *Virulence* **4**, 847–858. <https://doi.org/10.4161/viru.27172> (2013).
- Sarver, E., Keles, C. & Afrouz, S. G. Particle size and mineralogy distributions in respirable dust samples from 25 US underground coal mines. *Int. J. Coal Geol.* **247**, 103851. <https://doi.org/10.1016/j.coal.2021.103851> (2021).
- Pavan, C. et al. The puzzling issue of silica toxicity: are Silanols bridging the gaps between surface States and pathogenicity? *Part. Fibre Toxicol.* **16**, 32. <https://doi.org/10.1186/s12989-019-0315-3> (2019).
- Chen, W. et al. Risk of silicosis in cohorts of Chinese Tin and tungsten miners, and pottery workers (I): an epidemiological study. *Am. J. Ind. Med.* **48**, 1–9. <https://doi.org/10.1002/ajim.20174> (2005).

22. Creutzenberg, O. et al. Toxicity of a quartz with occluded surfaces in a 90-Day intratracheal instillation study in rats. *Inhalation Toxicol.* **20**, 995–1008. <https://doi.org/10.1080/08958370802123903> (2008).
23. Fubini, B. Surface chemistry and quartz hazard. *Ann. Occup. Hyg.* **42**, 521–530. [https://doi.org/10.1016/s0003-4878\(98\)00066-0](https://doi.org/10.1016/s0003-4878(98)00066-0) (1998).
24. Stone, V. et al. Effect of coal mine dust and clay extracts on the biological activity of the quartz surface. *Toxicol. Lett.* **149**, 255–259. <https://doi.org/10.1016/j.toxlet.2003.12.036> (2004).
25. Wallace, E. et al. Clay occlusion of respirable quartz particles detected by low voltage scanning electron microscopy — x-ray analysis. *Ann. Occup. Hyg.* **34**, 195–204. <https://doi.org/10.1093/annhyg/34.2.195> (1990).
26. Harrison, J. C. et al. Surface composition of respirable silica particles in a set of U.S. Anthracite and bituminous coal mine dusts. *J. Aerosol. Sci.* **28**, 689–696. [https://doi.org/10.1016/S0021-8502\(96\)00033-X](https://doi.org/10.1016/S0021-8502(96)00033-X) (1997).
27. Keles, C. & Sarver, E. A. Study of respirable silica in underground coal mines: particle characteristics. *Minerals* **12**, 1555 (2022).
28. Armbruster, L. in (eds Inhaled Particles, V. I., Dodgson, J., McCallum, R. I., Bailey, M. R. & Fisher, D. R.) 393–401 (Pergamon, (1988).
29. LaBranche, N., Teale, K., Wightman, E., Johnstone, K. & Cliff, D. Characterization analysis of airborne particulates from Australian underground coal mines using the mineral liberation analyser. *Minerals* **12**, 796 (2022).
30. Pandey, J. K. et al. Characterisation of respirable dust exposure of different category of workers in Jharia coalfields. *Arab. J. Geosci.* **10**, 183. <https://doi.org/10.1007/s12517-017-2974-4> (2017).
31. Su, X., Ding, R. & Zhuang, X. Characteristics of dust in coal mines in central North China and its research significance. *ACS Omega*. **5**, 9233–9250. <https://doi.org/10.1021/acsomega.0c00078> (2020).
32. Zazouli, M. A. et al. Physico-chemical properties and reactive oxygen species generation by respirable coal dust: implication for human health risk assessment. *J. Hazard. Mater.* **405**, 124185. <https://doi.org/10.1016/j.jhazmat.2020.124185> (2021).
33. Gonzalez, J., Keles, C., Sarver, E. & Mining On the Occurrence and Persistence of Coal-Mineral Microagglomerates in Respirable Coal Mine Dust. *Metall. Explor.* **39**, 271–282, doi:<https://doi.org/10.1007/s42461-022-00555-7> (2022).
34. Gonzalez, J., Keles, C., Pokhrel, N., Jaramillo, L. & Sarver, E. Respirable dust constituents and particle size: a case study in a thin-seam coal mine. *Min. Metall. Explor.* **39**, 1007–1015. <https://doi.org/10.1007/s42461-022-00611-2> (2022).
35. Pokhrel, N. et al. Comparison of Respirable Coal Mine Dust Constituents Estimated using FTIR, TGA, and SEM-EDX. *Metall. Explor.* **39**, 291–300, doi:<https://doi.org/10.1007/s42461-022-00567-3> (2022).
36. Johann-Essex, V., Keles, C., Sarver, E. A. & Computer-Controlled SEM-EDX routine for characterizing respirable coal mine dust. *Minerals* **7** (2017).
37. Keles, C., Taborda, M. J., Sarver, E. & Updating Characteristics of respirable dust in eight Appalachian coal mines: A dataset including particle size and mineralogy distributions, and metal and trace element mass concentrations with expanded data to cover a total of 25 US mines. *Data Brief.* **42**, 108125. <https://doi.org/10.1016/j.dib.2022.108125> (2022).
38. Mayeux, J. M., Kono, D. H. & Pollard, K. M. Development of experimental silicosis in inbred and outbred mice depends on instillation volume. *Sci. Rep.* **9**, 14190. <https://doi.org/10.1038/s41598-019-50725-9> (2019).
39. Pavan, C. et al. Nearly free surface Silanols are the critical molecular moieties that initiate the toxicity of silica particles. *Proc. Natl. Acad. Sci.* **117**, 27836–27846. <https://doi.org/10.1073/pnas.2008006117> (2020).
40. Keles, C., Pokhrel, N. & Sarver, E. A study of respirable silica in underground coal mines: sources. *Minerals* **12** (2022).
41. Ott, D. K. & Peters, T. M. A shelter to protect a passive sampler for coarse particulate matter, PM₁₀–2.5. *Aerosol Sci. Technol.* **42**, 299–309. <https://doi.org/10.1080/02786820802054236> (2008).
42. Greth, A., Afrouz, S., Keles, C. & Sarver, E. Characterization of respirable coal mine dust recovered from fibrous Polyvinyl chloride filters by scanning electron microscopy. *Min. Metall. Explor.* <https://doi.org/10.1007/s42461-024-00999-z> (2024).
43. Keles, C. & Sarver, E. Respirable silica particles in coal mine dust: an image library dataset collected using scanning electron microscopy with energy dispersive X-ray spectroscopy. *Data Brief.* **51**, 109656. <https://doi.org/10.1016/j.dib.2023.109656> (2023).
44. Sellaró, R., Sarver, E. & Baxter, D. A. Standard characterization methodology for respirable coal mine dust using SEM-EDX. *Resources* **4**, 939–957 (2015).
45. Jaramillo, L., Agioutanti, E., Ghaychi Afrouz, S., Keles, C. & Sarver, E. Thermogravimetric analysis of respirable coal mine dust for simple source apportionment. *J. Occup. Environ. Hyg.* **19**, 568–579. <https://doi.org/10.1080/15459624.2022.2100409> (2022).
46. Gui, X., Xing, Y., Rong, G., Cao, Y. & Liu, J. Interaction forces between coal and kaolinite particles measured by atomic force microscopy. *Powder Technol.* **301**, 349–355. <https://doi.org/10.1016/j.powtec.2016.06.026> (2016).
47. Zhang, R., Liu, S. & Zheng, S. Characterization of nano-to-micron sized respirable coal dust: particle surface alteration and the health impact. *J. Hazard. Mater.* **413**, 125447. <https://doi.org/10.1016/j.jhazmat.2021.125447> (2021).

Acknowledgements

The authors would like to thank our industry partners and mine personnel for arranging mine access and providing logistical support for dust sampling. Additionally, we acknowledge the Institute for Critical Technology and Applied Sciences' Nanoscale Characterization and Fabrication Laboratory (NCFL), which houses the SEM-EDX facilities used here. The NCFL is supported by the Virginia Tech National Center for Earth and Environmental Nanotechnology Infrastructure (NanoEarth), a member of the National Nanotechnology Coordinated Infrastructure (NNCI), supported by NSF (ECCS 1542100 and ECCS 2025151). Views expressed in this study are those of the authors and not necessarily the views of sponsors or research partners.

Author contributions

E.S. and C.K. conceptualized the research and designed the experimental methodology; C.K., D.S. and L.J. performed experiments and collected data; E.S. and D.S. wrote the main text of the manuscript; E.S. and D.S. prepared all figures; L.J. and C.K. reviewed and edited the main text of the manuscript; E.S. was responsible for project funding and administration. All authors have read and agreed to the published version of the manuscript.

Funding

The gratefully acknowledge the Centers for Disease Control, National Institute of Occupational Safety & Health (contracts 75D30122C14433 and 75D30119C05529) for funding this work.

Declarations

Competing interests

The authors declare no competing interests.

Additional information

Supplementary Information The online version contains supplementary material available at <https://doi.org/10.1038/s41598-025-01786-6>.

Correspondence and requests for materials should be addressed to E.S.

Reprints and permissions information is available at www.nature.com/reprints.

Publisher's note Springer Nature remains neutral with regard to jurisdictional claims in published maps and institutional affiliations.

Open Access This article is licensed under a Creative Commons Attribution-NonCommercial-NoDerivatives 4.0 International License, which permits any non-commercial use, sharing, distribution and reproduction in any medium or format, as long as you give appropriate credit to the original author(s) and the source, provide a link to the Creative Commons licence, and indicate if you modified the licensed material. You do not have permission under this licence to share adapted material derived from this article or parts of it. The images or other third party material in this article are included in the article's Creative Commons licence, unless indicated otherwise in a credit line to the material. If material is not included in the article's Creative Commons licence and your intended use is not permitted by statutory regulation or exceeds the permitted use, you will need to obtain permission directly from the copyright holder. To view a copy of this licence, visit <http://creativecommons.org/licenses/by-nc-nd/4.0/>.

© The Author(s) 2025